LIMNOLOGY AND OCEANOGRAPHY
Letters

ASLO
Open Access

Limnology and Oceanography Letters 9, 2024, 776–784

doi: 10.1002/lol2.10429

LETTER

Tagging of water masses with covariance of trace metals and prokaryotic taxa in the Southern Ocean

Rui Zhang[1], *Stéphane Blain*[1], *Corentin Baudet*[2], *Hélène Planquette*[2], *Frédéric Vivier*[3], *Philippe Catala*[1], *Olivier Crispi*[1], *Audrey Guéneuguès*[1], *Barbara Marie*[1], *Pavla Debeljak*[4,5], *Ingrid Obernosterer*[1]*

[1]CNRS, Sorbonne Université, Laboratoire d'Océanographie Microbienne, LOMIC, Banyuls-sur-mer, France; [2]Université Bretagne Occidentale, CNRS, IRD, Ifremer, UMR 6539, LEMAR, Plouzané, France; [3]LOCEAN-IPSL, CNRS, Sorbonne Université, Paris, France; [4]Supbiotech, Villejuif, France; [5]Sorbonne Université, Muséum National d'Histoire Naturelle, CNRS, EPHE, Université des Antilles, Institut de Systématique, Evolution, Biodiversité (ISYEB), Paris, France

Scientific Significance Statement

Marine microorganisms require major and minor nutrients to thrive in the ocean. The spatial distribution of microorganisms and their resources is strongly influenced by ocean circulation and therefore the distribution of water masses. Based on a large dataset collected in the Indian Sector of the Southern Ocean, we performed a statistical co-analysis of the heterotrophic microbial community composition and the distribution of their resources including trace metals. Although the interplay between microorganisms and nutrients is complex, clear biogeochemical signatures of water masses emerge from this analysis. For the first time, large-scale covariations of trace metals and microbial taxa are revealed. These allow to mark water masses from a novel perspective and pave the way for further research into the underlying microbial mechanism.

Abstract

Marine microbes are strongly interrelated to trace metals in the ocean. How the availability of trace metals selects for prokaryotic taxa and the potential feedback of microbial processes on the trace metal distribution in the ocean remain poorly understood. We investigate here the potential reciprocal links between diverse prokaryotic taxa and iron (Fe), manganese (Mn), copper (Cu), and nickel (Ni) as well as apparent oxygen utilization (AOU) across 12 well-defined water masses in the Southern Indian Ocean (*SWINGS—South West Indian Ocean*

*Correspondence: ingrid.obernosterer@obs-banyuls.fr

[Correction added on September 21, 2024, after initial online publication: For the co-author "Pavla Debeljak", the affiliation "Supbiotech, Villejuif, France" missed incorrectly earlier has been added as the first affiliation in this version. The first affiliation which is already available is repositioned as second affiliation.]

Associate editor: Hugo Sarmento

Author Contribution Statement: RZ, SB, and IO designed the research. Sampling was performed by RZ and IO. DNA extraction and bioinformatic analysis were performed by RZ. Data analyses were carried out by RZ, SB, and P.D, and IO, CB, and HP provided the trace metal data. Water masses were identified by FV. PC, OC, AG, BM, and SB collected samples and provided the data of cell abundance, major nutrients, and DOC. RZ, SB, and IO wrote the first draft of the manuscript. All authors contributed to editing the manuscript.

Data Availability Statement: The datasets generated and analyzed during the current study are available in the European Nucleotide Archive (ENA) repository at https://www.ebi.ac.uk/ena under the project ID PRJEB63680. Environmental and biogeochemical data are available under doi: https://doi.org/10.17882/99983.

Additional Supporting Information may be found in the online version of this article.

GEOTRACES GS02 Section cruise). Applying partial least square regression (PLSR) analysis, we show that the water masses are associated with particular latent vectors that are a combination of the spatial distribution of prokaryotic taxa, trace elements, and AOU. This approach provides novel insights on the potential interactions between prokaryotic taxa and trace metals in relation to organic matter remineralization in distinct water masses of the ocean.

The ocean is a dynamical system where hydrological features shape the seascape at multiple scales (Kavanaugh et al. 2014). Hydrographically defined water masses can constrain biogeochemical processes, resulting in vertical or horizontal gradients of major nutrients and trace metals (Jenkins et al. 2015). In parallel, the composition of microbial communities that are key mediators in nutrient cycling varies among ocean basins and along geographical ranges and depth layers (Galand et al. 2010; Agogué et al. 2011; Salazar et al. 2016; Raes et al. 2018; Sow et al. 2022). Frontal systems, upwelling and mesoscale eddies can structure community composition on a regional scale (Baltar et al. 2010; Lekunberri et al. 2013; Hernando-Morales et al. 2017). Specific hydrographic and biogeochemical properties, such as the concentration of major nutrients, were identified as factors with potential reciprocal influence on these biogeographic patterns in the ocean (Hanson et al. 2012).

Trace metals, such as iron (Fe), manganese (Mn), nickel (Ni), and copper (Cu), play crucial roles in microbial growth and metabolism (Morel and Price 2003) and are therefore important micronutrients (Lohan and Tagliabue 2018). In heterotrophic prokaryotes, Fe is essential in the respiratory chain (Andrews et al. 2003); thus, Fe availability affects the processing of organic carbon (Fourquez et al. 2014). Mn (II) serves as a cofactor for various enzymes involved in the central carbon metabolism and in antioxidant activity (Hansel 2017). Ni has been identified as an indispensable element for nitrogen fixation (Glass and Dupont 2017) and for chemolithotrophic prokaryotes (Gikas 2008). Cu acts as a cofactor for numerous proteins involved in redox reactions, oxidative respiration, denitrification, and other processes (Argüello et al. 2013). Cu deficiency can affect microbial growth, but certain concentrations of dissolved Cu can also be toxic to heterotrophic prokaryotes or phytoplankton in the ocean (Moffett et al. 1997; Debelius et al. 2011; Posacka et al. 2019).

The biological roles of Fe, Ni, and Cu result in nutrient-like vertical profiles in the offshore ocean with low concentrations in surface waters due to biological uptake by autotrophic and heterotrophic microbes and increases with depth due to remineralization of sinking material. The magnitude of these uptake and remineralization processes is tightly linked to the composition of the microbial community and its metabolic capabilities. The expected nutrient-like profile is not observed for Mn due to the photoproduction of the soluble form of Mn (II) in surface waters and the biologically mediated production of insoluble MnO_x at depth (Sunda et al. 1983). Adding to this complexity, transport and mixing largely influence the large-scale distribution of these trace metals (Thi Dieu Vu and Sohrin 2013; Latour et al. 2021; Chen et al. 2023). The GEOTRACES program has made major advances in the determination of the trace metal content of water masses across the global ocean, but the interplay with the microbial community remains to date poorly understood. In this context, the main objective of the present study was to investigate the potential interactive effect between trace elements and microbes, and how these could influence chemical and biological water-mass-specific properties across 12 well-defined water masses in the Southern Indian Ocean (*SWINGS—South West Indian Ocean Geotraces Section cruise, GEOTRACES GS02* section).

Materials and methods

Environmental context

Samples were collected during the *SWINGS* cruise between January 10, 2021 and March 8, 2021. The 23 stations sampled for the present study (Fig. 1A) were located in the Subtropical Zone (STZ), Subantarctic Zone (SAZ), the Polar Frontal Zone (PFZ), and the Antarctic Zone (AAZ). Surface water (20 m) sampled at each of these stations is assigned to these geographical zones, and the samples below the mixed layer were categorized into 12 water masses according to their physicochemical properties (Fig. 1B). Water masses were identified at each station from the vertical profile of physical properties (Supplementary Fig. S1; Table S1) and geographical considerations. The details are described in the Supplementary Methods.

All seawater samples dedicated to microbial community composition were collected using 12-liter Niskin bottles mounted on a rosette equipped with conductivity, temperature, and depth (CTD) sensors (SeaBird SBE911plus). Seawater (6 liters) was sequentially passed through 0.8-μm polycarbonate (PC) filters (47 mm diameter, Nuclepore, Whatman, Sigma-Aldrich) and 0.22-μm Sterivex filter units (Sterivex, Millipore, EMD). The cells concentrated on the 0.8-μm filters were considered particle attached (PA) and those on the 0.22-μm filters as free living (FL). The filters were stored at −80°C until returned to the home laboratory for DNA extraction. Sample collection, preservation, and analyses of major nutrients, trace elements, and dissolved oxygen were determined using standard protocols and are described in the Supplementary Methods, and data are available under doi: https://doi.org/10.17882/99983.

DNA extraction and sequencing

Total DNA was extracted from the 0.8-μm filters and the 0.22-μm Sterivex filter units using the DNeasy PowerWater Kit (Qiagen) according to the manufacturer's instructions with a

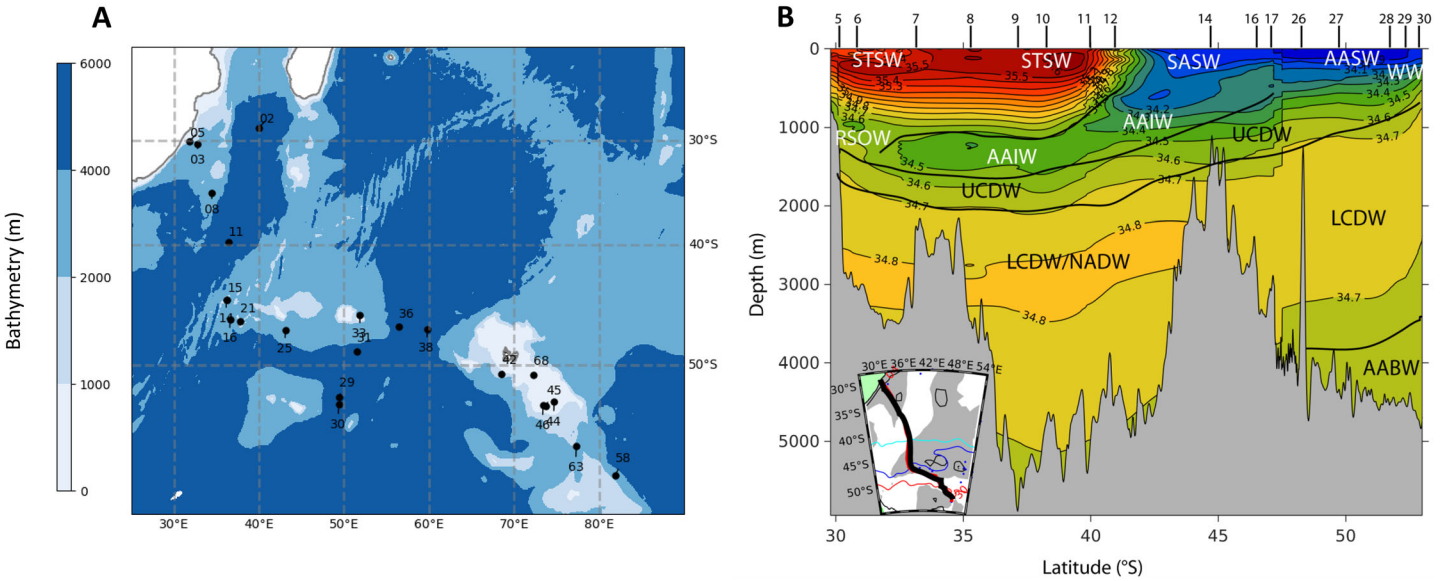

Fig. 1. (**A**) Map of stations sampled for the present study during the *SWINGS* cruise in the Indian Sector of the Southern Ocean. Color shading represents bathymetry and the gray line contours South Africa (25°–35°E) and Madagascar (45°–50°E). Subtropical Zone (STZ) (Stas. 2, 3, 5, 8, and 11), Subantarctic Zone (SAZ) (Stas. 14, 15, 16, 38), the Polar Frontal Zone (PFZ) (Stas. 21, 25, 31, 33, and 36), and the Antarctic Zone (AAZ) (Stas. 29, 30, 42, 44, 45, 46, 58, 63, and 68). (**B**) A cross-section (inserted map) showing the vertical distribution of some water masses sampled at the stations indicated on the upper *x*-axis. Lines indicate salinity. The full list of water masses is provided in Fig. 2. AABW, Antarctic Bottom Water; AAIW, Antarctic Intermediate Water; ASW, Antarctic Surface Water; LCDW, Lower Circumpolar Deep Water; LCDW/NADW, Lower Circumpolar Deep Water/ North Atlantic Deep Water; RSOW, Red Sea Overflow Water; SASW, Sub-Antarctic surface water; STSW, Subtropical Surface Water; UCDW, Upper Circumpolar Deep Water; WW, Winter Water.

few modifications described in the Supplementary Methods. The V4–V5 region of the 16S rRNA gene was amplified with primers as described previously (Liu et al. 2020). 16S rRNA gene amplicons were sequenced with Illumina MiSeq V3 2 × 300 bp chemistry at the platform Biosearch Technologies (Berlin, Germany). Data are available in the European Nucleotide Archive (ENA) repository at https://www.ebi.ac.uk/ena under the project ID PRJEB63680.

Data analysis

16S rRNA gene sequences were demultiplexed using the Illumina bcl2fastq v2.20 at the platform Biosearch Technologies. The PCR primers and adapters of 16S rRNA gene sequences were trimmed with cutadapt v1.15 (Martin 2011). Amplicon sequencing variants (ASVs) were produced in R using DADA2 package (v1.24) (Callahan et al. 2016) with the following parameters: truncLen = *c*(240, 210), max*N* = 0, maxEE = *c*(3, 5), truncQ = 2. This pipeline includes the following steps: filter and trim, dereplication, sample inference, merge paired reads, and chimera removal. A total of 12,847 unique amplicon sequence variants (ASVs) were obtained from the 172 samples collected (FL and PA prokaryotes combined). Taxonomic assignment of ASVs was performed using the DADA2-formatted SILVA SSU Ref NR99 138 database (Quast et al. 2012). The number of reads per sample varied between 2633 and 241,954. Singletons and sequences belonging to eukaryotes, chloroplasts, and mitochondria were removed. To obtain the same number of reads for all samples, the dataset was randomly subsampled to 4493 reads per sample with the function rarefy_even_depth by the Phyloseq package (v1.40) (McMurdie and Holmes 2013) in R. After subsampling 10,138 ASVs were obtained in total, of which 5847 ASVs from the FL fraction ($n = 76$) and 6461 ASVs from the PA fraction ($n = 80$).

All statistical analyses were performed using the R 4.2.1 version. Nonmetric dimensional scaling (NMDS) ordinations were generated based on Bray–Curtis dissimilarity (Legendre and Gallagher 2001) using the ordinate function in the Phyloseq package. Analysis of similarity (ANOSIM) was performed via the vegan package (v2.6) (Dixon 2003) to test for significant differences in microbial communities between water masses. To test the association of the FL prokaryotic community composition and environmental factors, partial least squares regression (PLSR) (Guebel and Torres 2013) analysis with cross-validation was performed using pls v2.8 package (Mevik and Wehrens 2007) in R with the relative abundance of abundant ASVs as the *Y* variables and the environmental factors as the *X* variables (data are available under doi: https://doi.org/10.17882/99983). Scale transformation of the data matrix was performed to standardize before data input to the model. The regression coefficients were extracted with the function coef by the pls package in R. For the

identification of indicator ASVs for surface waters and deep-water masses, the IndVal index from the labdsv package (v2.0) (Roberts 2019) in R was used. This index takes into account the specificity, fidelity, and relative abundance of the ASVs in the different water masses and surface waters.

Results and discussion

Structuring of microbial communities by water masses

In surface waters, microbial communities clustered according to geographical zone and frontal system, and in the subsurface, the clustering was driven by water mass (Fig. 2). This spatial structuring was significant for both FL (ANOSIM, $R = 0.8651$, $p = 0.0001$) and PA communities (ANOSIM, $R = 0.714$, $p = 0.0001$). Hierarchical clustering dendrograms further illustrate a structuring effect of water masses for FL and PA microbial communities (Supplementary Fig. S2). For a given water mass, the composition of the microbial communities was, however, significantly different between size fractions (Supplementary Figs. S3–S5; Supplementary Results), suggesting that factors that are dependent and independent of size fraction together influence the observed biogeographical patterns. Particles are known to host distinct communities, and the nature of the particles can shape the associated prokaryotic assemblages (Baumas and Bizic 2024). Sinking particles were suggested to act as vectors for microbes across the water column (Mestre et al. 2018), an idea that is supported by the about twofold lower number of indicator species for a given water mass for the PA (121) as compared to the FL (213) communities (Supplementary Fig. S6; Tables S2–S3; Supplementary Results). Taken together, these observations point to a complex interplay between processes specific to the particle sphere and habitat-type independent factors, such as temperature or hydrostatic pressure, to shape the prokaryotic community composition.

Microbial "biogeo"-gradients

Identifying the factors that select for microbial taxa and understanding the potential feedback of microbes on the biogeochemical properties of the water mass they thrive in remains challenging. In this context, the role of trace elements in the ocean interior has, to the best of our knowledge, never been considered. To explore the potential reciprocal links between environmental and microbial parameters, we used PLSR. PLSR is a multivariate regression model based on a simultaneous PCA on two matrices, which achieves the best relationships between them (Dunn 2020). An advantage of PLSR is that it prevents the bias of colinearity, a facet not taken into consideration by PCA. PLSR has been successfully applied to determine the ecological vectors associated with carbon flux or trace metal export (Rembauville et al. 2015; Blain et al. 2022), to predict the partitioning of carbon among

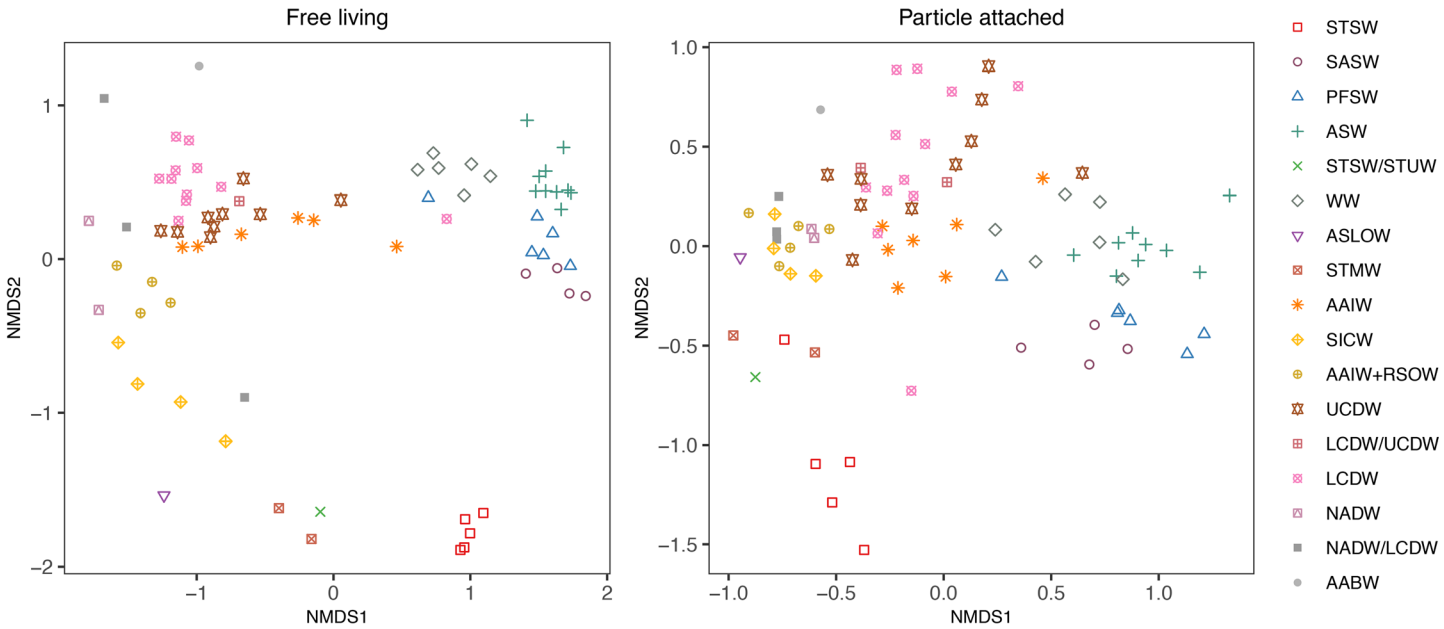

Fig. 2. Nonmetric multidimensional scaling (NMDS) plots of free-living (FL) and particle-attached (PA) prokaryotic communities based on Bray–Curtis dissimilarity. ANOSIM statistics: FL, *R*: 0.8651, significance: 1*e*-04; PA, *R*: 0.714, significance: 1*e*-04. AABW, Antarctic Bottom Water; AAIW, Antarctic Intermediate Water; AAIW + RSOW, Antarctic Intermediate Water mixed with Red Sea Overflow Water; ASLOW, Arabian Sea Low-Oxygen Water; ASW, Antarctic Surface Water; LCDW/UCDW, Lower Circumpolar Deep Water/Upper Circumpolar Deep Water; NADW, North Atlantic Deep Water; LCDW, Lower Circumpolar Deep Water; NADW/LCDW, North Atlantic Deep Water/Lower Circumpolar Depp Water; PFSW, Polar Frontal Surface water; SASW, Sub-Antarctic Surface Water; SICW, South Indian Central Water; STMW, Subtropical Mode Water; STSW, Subtropical Surface Water; STUW, Subtropical Underwater; STSW/STUW, Subtropical Surface Water/Subtropical Underwater; UCDW, Upper Circumpolar Deep Water; WW, Winter Water.

microbial community members based on bio-optical properties (Rembauville et al. 2017), or to link biodiversity and carbon fluxes (Guidi et al. 2016). We carried out PLSR using only those available environmental parameters for which a reciprocal influence can be expected, which are the concentrations of the major nutrients nitrate (NO_3^-) and phosphate (PO_4^{3-}), the trace elements manganese (Mn), iron (Fe), nickel (Ni), and copper (Cu), and apparent oxygen utilization (AOU). We considered only ASVs with a relative abundance of ≥ 5% in at least one sample (22 ASVs; Table S4) as abundant taxa are expected to dominate the interplay with nutrients in different water masses. To confirm this idea, we also performed a PLSR analysis with ASVs with a relative abundance of ≥ 1%. We carried out the PLSR analysis with ASVs in the free-living fraction, because the concentrations of major and trace nutrients were only available in the dissolved phase.

The PLSR analysis revealed that the three first latent vectors explained 61%, 16%, and 9% of the covariance (Fig. 3A,B; Supplementary Fig. S7). Therefore, any sample associated with a water mass, which was initially described by 29 variables (7 environmental factors and 22 ASVs), can now be described in a three-dimensional space. This reduction in complexity facilitates the examination of whether water masses are associated with particular latent vectors, which we propose to call microbial "biogeo"-gradients (BG). These BGs are a combination of the spatial distribution of environmental factors and ASVs. Our results show that BG1 discriminates deep, cold-water masses (UCDW, LCDW, AAIW) (negative signs) from warmer and more saline subtropical waters (STSW/STUW, STMW, ASLOW) (positive signs) (Fig. 3C,D). BG2 mainly discriminates WW (negative sign) (Fig. 3C,E). BG3 provides a partitioning between NADW/LCDW and WW (positive sign) and AAIW and UCDW (negative sign) (Fig. 3C,F). The PLSR analysis performed with ASVs ≥ 1% relative abundance (246 ASVs) confirmed this result, as the ASVs with < 5% relative abundance are close to the origin of the latent vector space and thus do not have a strong discriminative power (Supplementary Fig. S8).

Physical properties of water masses are set by the conditions at the formation and the subsequent transport and mixing in the ocean interior. These abiotic processes, together with additional biotic transformations, contribute to structure on the one hand the distribution of environmental parameters (Supplementary Figs. S9–S11; data are available under doi:

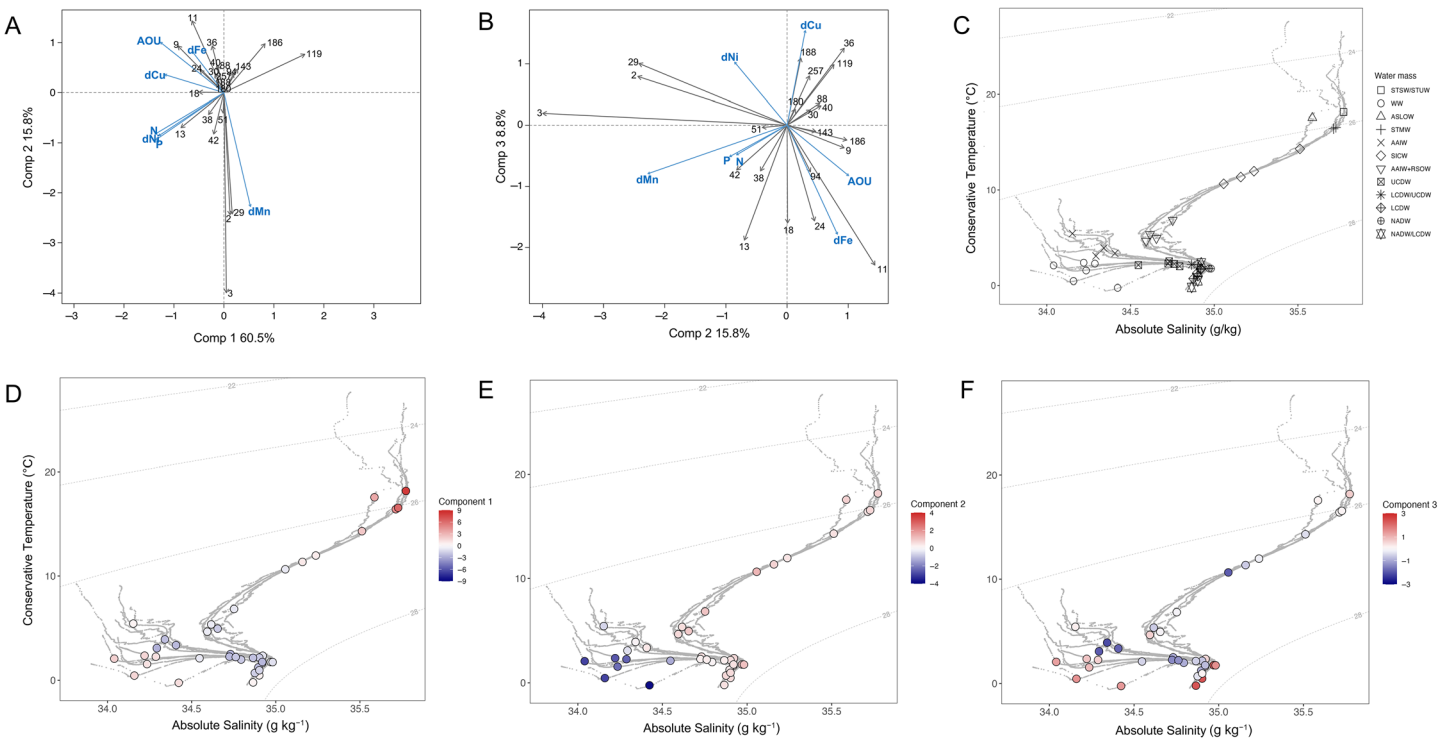

Fig. 3. (**A**) Partial least squares regression (PLSR) analysis linking abundant ASVs (relative abundance ≥ 5% in at least one sample) with environmental variables. Blue labels describe the environmental variables (AOU, apparent oxygen utilization; P, phosphate; N, nitrate; dMn, dissolved manganese; dFe, dissolved iron; dNi, dissolved nickel; dCu, dissolved copper), whereas gray labels describe the ASVs (detailed in Fig. 4). Shown are components 1 and 2. (**B**) Components 2 and 3 of the PLSR analysis. (**C**) Temperature–salinity diagram and localization of samples collected in different water masses and used for PLSR. (**D**) Temperature–salinity diagram and localization of samples. The color coding corresponds to the first component of scores of samples extracted from PLSR. (**E**) As for (**C**), but the color coding corresponds to the second component of scores of samples extracted from PLSR. (**F**) As for (**C**), but the color coding corresponds to the third component of scores of samples extracted from PLSR.

https://doi.org/10.17882/99983) and on the other hand the distribution of prokaryotic taxa as discussed above (Supplementary Figs. S4–S5 and S12). Our observations that BGs are good descriptors of water masses suggest that they provide clues on the possible interactions between environmental factors and prokaryotic taxa that together contribute to the structuring of latent vectors in the three-dimensional space.

We discuss in the following these possible reciprocal feedbacks that are the basis of the nature of the BGs. BG1 is dominated by processes linked to remineralization, as indicated by the contribution of AOU (Fig. 3A). Therefore, the gradients of the other contributors to BG1 (Fe, Cu, N, P, Ni, and ASVs) across different water masses could be related to this process. Our analysis highlights several ASVs (9, 11, 13, 18, 24) as potential key drivers of remineralization processes (Fig. 3A). BG2 has a more complex structure because it is defined as a gradient with opposite trends between Fe, AOU, and the related ASVs (9, 11, 24) and Mn, N, P, and Ni and the related ASVs (2, 3, 29). BG3 captures contrasted conditions with opposite gradients between Fe, AOU, and the associated ASVs (9, 11, 13, 18, 24, 94), and Ni and Cu associated with another group of ASVs (36, 119, 188, 257) (Fig. 3B; Supplementary Fig. S7).

All three BGs are related to remineralization, an observation that is not surprising as this process occurs in all water masses. The regression coefficients, which summarize the information contained in the different BGs, reveal 12 ASVs with a positive relationship with AOU (Fig. 4). The concurrently positive regression coefficients of these ASVs with Fe could indicate that either this element stimulates their metabolic activity and contribution to remineralization or the enhanced supply of Fe by these microbial taxa through remineralization. However, these ASVs could further be partitioned into different groups, revealing that Cu is potentially an important discriminating factor. One group of ASVs

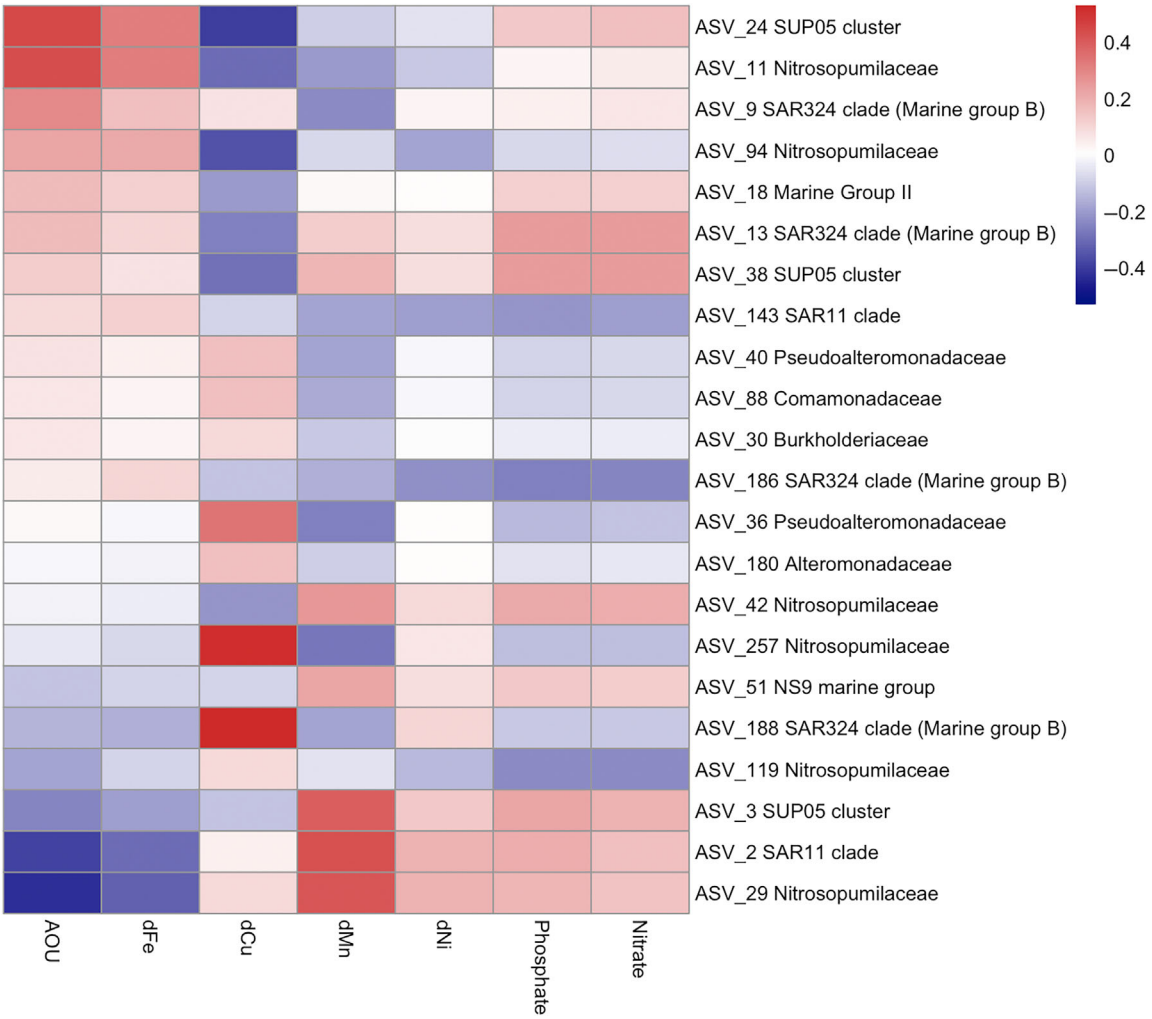

Fig. 4. Heatmap based on the regression coefficients of abundant free-living prokaryotes (relative abundance of ASVs ≥ 5% in at least one sample) and environmental variables. The regression coefficients are extracted from the PLSR model.

(11, 13, 18, 24, 38, 94) thrives in low Cu conditions, while another group of ASVs (ASV 9, 30, 40, 88) accommodates with high Cu concentrations. This observation could suggest that the group with negative regressions is either sensitive to the toxicity of Cu or that these ASVs extensively use Cu. Consequently, ASVs belonging to this latter group are potential contributors to the remineralization of Cu.

Negative regression coefficients with AOU were observed with several ASVs, suggesting that their activity is decoupled from the remineralization of organic matter. Among these, three ASVs (2, 3, 29) had positive regression coefficients with Mn and, to a lesser extent, with N, P, and Ni. These ASVs were highlighted by BG2 that tags WW (Fig. 3E), young water masses with low AOU, typical of HNLC-type waters with high concentrations of N, P and low concentrations of Fe. In the case of Mn, the prokaryotic-mediated oxidation of Mn (II) to insoluble Mn (IV) can lead to low Mn concentrations, whereas photoinduced, organically mediated reduction of Mn (IV, III) can result in high concentrations of this trace element in surface waters (Sunda and Huntsman 1994). This could pinpoint the ASVs with negative regression coefficients (257, 188, and 119) as potential mediators of this reduction (Jones et al. 2020). Another group of ASVs (36, 119, 188, 257) revealed positive regression coefficients with Cu and were significant contributors to BG3, a good marker of NADW/LCDW. The absence of positive regression coefficients with AOU suggests that these ASVs are not Cu remineralizers, but that they are able to thrive in high Cu concentrations ($\sim$ 1.7 nM in NADW and LCDW). This group also contains ASVs that have high negative regression coefficients with Mn.

Our data provide novel insights on the potential interactions between abundant ASVs and trace metals in relation to organic matter remineralization. Among these ASVs, only seven ASVs were detected by the indicator species analysis (Supplementary Fig. S6), illustrating the potential of PLSR analysis to identify key microbes if combined with appropriate biogeochemical parameters. Together, these results provide a new view on the parallel distribution of biogeochemical variables and prokaryotic taxa in distinct water masses. Because our results are based on the ASV level, the limited functional knowledge does not allow us to infer the specific pathways involved in trace element cycling by these prokaryotes. However, our results provide the opportunity to identify testable hypotheses on the underlying mechanisms, as illustrated for a few specific taxa below.

We observed that distinct ASVs belonging to the same family revealed opposite regression coefficients with trace elements. This was the case, for example, of ASVs belonging to *Nitrosopumilaceae*. Although ASV 11 and 94 had positive regression coefficients with Fe and negative ones with Cu, ASV 29 and 119 revealed the opposite patterns. *Nitrosopumilaceae* are well-known chemolithoautotrophic ammonia oxidizers (Qin et al. 2016), but this family also contains members with heterotrophic metabolism (Pester et al. 2011; Aylward and Santoro 2020). Fe and Cu availability appears to shape the ecological niches of different strains belonging to this group (Shafiee et al. 2019, 2021). A similar differentiation was observed for ASVs of the SUP05 cluster (ASV 24 and 38 vs. ASV 3). Strong positive regressions with Cu were further detected for ASV188 (SAR324 clade, Marine Group B), ASV 36 (*Pseudoalteromonadaceae*), and ASV 188 (*Alteromonadacea*). Culture work revealed a range of physiological responses and consequences on cellular carbon metabolism among diverse bacterial strains to Cu gradients (Posacka et al. 2019), illustrating that the requirements of this trace metal or the sensitivities toward its toxicity are highly variable. Insights on the contrasting interplays between trace metals and prokaryotic taxa, including closely related ones, could be gained through the investigation of the gene inventories of the metabolic pathways of interest. Quantifying the genes of the respective transporters as well as of metabolisms involving trace elements in the water masses where these taxa are abundant and describing the gene repertoire of representative MAGs could be a possible way to further investigate the ecological niches of ASVs in relation to trace metals in future studies.

References

Agogué, H., D. Lamy, P. R. Neal, M. L. Sogin, and G. J. Herndl. 2011. Water mass-specificity of bacterial communities in the North Atlantic revealed by massively parallel sequencing: Bacterial assemblages in North Atlantic Ocean. Mol. Ecol. **20**: 258–274. doi:10.1111/j.1365-294X.2010.04932.x

Andrews, S. C., A. K. Robinson, and F. Rodríguez-Quiñones. 2003. Bacterial iron homeostasis. FEMS Microbiol. Rev. **27**: 215–237. doi:10.1016/S0168-6445(03)00055-X

Argüello, J. M., D. Raimunda, and T. Padilla-Benavides. 2013. Mechanisms of copper homeostasis in bacteria. Front. Cell. Infect. Microbiol. **3**: 73. doi:10.3389/fcimb.2013.00073

Aylward, F. O., and A. E. Santoro. 2020. Heterotrophic Thaumarchaea with small genomes are widespread in the dark ocean. mSystems **5**: e00415-20. doi:10.1128/mSystems.00415-20

Baltar, F., J. Arístegui, J. M. Gasol, I. Lekunberri, and G. J. Herndl. 2010. Mesoscale eddies: Hotspots of prokaryotic activity and differential community structure in the ocean. ISME J. **4**: 975–988. doi:10.1038/ismej.2010.33

Baumas, C., and M. Bizic. 2024. A focus on different types of organic matter particles and their significance in the open ocean carbon cycle. Prog Oceanogr. 224: 103233. https://doi.org/10.1016/j.pocean.2024.103

Blain, S., H. Planquette, I. Obernosterer, and A. Guéneuguès. 2022. Vertical flux of trace elements associated with lithogenic and biogenic carrier phases in the Southern Ocean. Global Biogeochem. Cycles **36**: e2022GB007371. doi:10.1029/2022GB007371

Callahan, B. J., P. J. McMurdie, M. J. Rosen, A. W. Han, A. J. A. Johnson, and S. P. Holmes. 2016. DADA2: High-resolution sample inference from Illumina amplicon data. Nat. Methods **13**: 581–583. doi:10.1038/nmeth.3869

Chen, X.-G., and others. 2023. Ocean circulation and biological processes drive seasonal variations of dissolved Al, Cd, Ni, Cu, and Zn on the Northeast Atlantic continental margin. Mar. Chem. **252**: 104246. doi:10.1016/j.marchem.2023.104246

Debelius, B., J. M. Forja, and L. M. Lubián. 2011. Toxicity of copper, nickel and zinc to Synechococcus populations from the Strait of Gibraltar. J. Mar. Syst. **88**: 113–119. doi:10.1016/j.jmarsys.2011.02.009

Dixon, P. 2003. VEGAN, a package of R functions for community ecology. J. Veg. Sci. **14**: 927–930. doi:10.1111/j.1654-1103.2003.tb02228.x

Dunn, K. 2020. Process improvement using data. Available from https://learnche.org/pid/PID.pdf?10d109.

Fourquez, M., A. Devez, A. Schaumann, A. Guéneuguès, T. Jouenne, I. Obernosterer, and S. Blain. 2014. Effects of iron limitation on growth and carbon metabolism in oceanic and coastal heterotrophic bacteria. Limnol. Oceanogr. **59**: 349–360. doi:10.4319/lo.2014.59.2.0349

Galand, P. E., M. Potvin, E. O. Casamayor, and C. Lovejoy. 2010. Hydrography shapes bacterial biogeography of the deep Arctic Ocean. ISME J. **4**: 564–576. doi:10.1038/ismej.2009.134

Gikas, P. 2008. Single and combined effects of nickel (Ni(II)) and cobalt (Co(II)) ions on activated sludge and on other aerobic microorganisms: A review. J. Hazard. Mater. **159**: 187–203. doi:10.1016/j.jhazmat.2008.02.048

Glass, J. B., and C. L. Dupont. 2017. Oceanic nickel biogeochemistry and the evolution of nickel use, p. 12–26. *In* D. Zamble, M. Rowińska-Żyrek, and H. Kozlowski [eds.], *The biological chemistry of nickel*. The Royal Society of Chemistry. doi.org/10.1039/9781788010580-00012

Guebel, D. V., and N. V. Torres. 2013. Partial least-squares regression (PLSR), p. 1646–1648. *In* W. Dubitzky, O. Wolkenhauer, K.-H. Cho, and H. Yokota [eds.], *Encyclopedia of systems biology*. Springer. doi.org/10.1007/978-1-4419-9863-7_1274

Guidi, L., and others. 2016. Plankton networks driving carbon export in the oligotrophic ocean. Nature **532**: 465–470. doi:10.1038/nature16942

Hansel, C. M. 2017. Manganese in marine microbiology, p. 37–83. *In* R. K. Poole and D. J. Kelly [eds.], *Advances in microbial physiology*. Elsevier. doi:10.1016/bs.ampbs.2017.01.005

Hanson, C. A., J. A. Fuhrman, M. C. Horner-Devine, and J. B. H. Martiny. 2012. Beyond biogeographic patterns: Processes shaping the microbial landscape. Nat. Rev. Microbiol. **10**: 497–506. doi:10.1038/nrmicro2795

Hernando-Morales, V., J. Ameneiro, and E. Teira. 2017. Water mass mixing shapes bacterial biogeography in a highly hydrodynamic region of the Southern Ocean: Water mixing shapes bacterial biogeography. Environ. Microbiol. **19**: 1017–1029. doi:10.1111/1462-2920.13538

Jenkins, W. J., W. M. Smethie, E. A. Boyle, and G. A. Cutter. 2015. Water mass analysis for the U.S. GEOTRACES (GA03) North Atlantic sections. Deep-Sea Res. II Top. Stud. Oceanogr. **116**: 6–20. doi:10.1016/j.dsr2.2014.11.018

Jones, M. R., G. W. Luther, and B. M. Tebo. 2020. Distribution and concentration of soluble manganese(II), soluble reactive Mn(III)-L, and particulate MnO_2 in the Northwest Atlantic Ocean. Mar. Chem. **226**: 103858. doi:10.1016/j.marchem.2020.103858

Kavanaugh, M. T., B. Hales, M. Saraceno, Y. H. Spitz, A. E. White, and R. M. Letelier. 2014. Hierarchical and dynamic seascapes: A quantitative framework for scaling pelagic biogeochemistry and ecology. Prog. Oceanogr. **120**: 291–304. doi:10.1016/j.pocean.2013.10.013

Latour, P., and others. 2021. Manganese biogeochemistry in the Southern Ocean, from Tasmania to Antarctica. Limnol. Oceanogr. **66**: 2547–2562. doi:10.1002/lno.11772

Legendre, P., and E. D. Gallagher. 2001. Ecologically meaningful transformations for ordination of species data. Oecologia **129**: 271–280. doi:10.1007/s004420100716

Lekunberri, I., E. Sintes, D. De Corte, T. Yokokawa, and G. J. Herndl. 2013. Spatial patterns of bacterial and archaeal communities along the Romanche Fracture Zone (tropical Atlantic). FEMS Microbiol. Ecol. **85**: 537–552. doi:10.1111/1574-6941.12142

Liu, Y., S. Blain, O. Crispi, M. Rembauville, and I. Obernosterer. 2020. Seasonal dynamics of prokaryotes and their associations with diatoms in the Southern Ocean as revealed by an autonomous sampler. Environ. Microbiol. **22**: 3968–3984. doi:10.1111/1462-2920.15184

Lohan, M. C., and A. Tagliabue. 2018. Oceanic micronutrients: Trace metals that are essential for marine life. Elements **14**: 385–390. doi:10.2138/gselements.14.6.385

Martin, M. 2011. Cutadapt removes adapter sequences from high-throughput sequencing reads. EMBnet J. **17**: 10. doi:10.14806/ej.17.1.200

McMurdie, P. J., and S. Holmes. 2013. phyloseq: An R package for reproducible interactive analysis and graphics of microbiome census data. PLoS One **8**: e61217. doi:10.1371/journal.pone.0061217

Mestre, M., C. Ruiz-González, R. Logares, C. M. Duarte, J. M. Gasol, and M. M. Sala. 2018. Sinking particles promote vertical connectivity in the ocean microbiome. Proc. Natl. Acad. Sci. USA **115**: E6799–E6807. doi:10.1073/pnas.1802470115

Mevik, B.-H., and R. Wehrens. 2007. The pls package: Principal component and partial least squares regression in *R*. J. Stat. Soft. **18**: 1–23. doi:10.18637/jss.v018.i02

Moffett, J. W., L. E. Brand, P. L. Croot, and K. A. Barbeau. 1997. Cu speciation and cyanobacterial distribution in harbors subject to anthropogenic Cu inputs.

Limnol. Oceanogr. **42**: 789–799. doi:10.4319/lo.1997.42.5.0789

Morel, F. M. M., and N. M. Price. 2003. The biogeochemical cycles of trace metals in the oceans. Science **300**: 944–947. doi:10.1126/science.1083545

Pester, M., C. Schleper, and M. Wagner. 2011. The Thaumarchaeota: An emerging view of their phylogeny and ecophysiology. Curr. Opin. Microbiol. **14**: 300–306. doi:10.1016/j.mib.2011.04.007

Posacka, A. M., D. M. Semeniuk, and M. T. Maldonado. 2019. Effects of copper availability on the physiology of marine heterotrophic bacteria. Front. Mar. Sci. **5**: 523. doi:10.3389/fmars.2018.00523

Qin, W., W. Martens-Habbena, J. N. Kobelt, and D. A. Stahl. 2016. *Candidatus* Nitrosopumilaceae, p. 1–2. *In* W. B. Whitman [ed.], *Bergey's manual of systematics of archaea and bacteria*. Wiley. doi:10.1002/9781118960608.fbm00262

Quast, C., E. Pruesse, P. Yilmaz, J. Gerken, T. Schweer, P. Yarza, J. Peplies, and F. O. Glöckner. 2012. The SILVA ribosomal RNA gene database project: Improved data processing and web-based tools. Nucleic Acids Res. **41**: D590–D596. doi:10.1093/nar/gks1219

Raes, E. J., and others. 2018. Oceanographic boundaries constrain microbial diversity gradients in the South Pacific Ocean. Proc. Natl. Acad. Sci. U. S. A. **115**: E8266–E8275. doi:10.1073/pnas.1719335115

Rembauville, M., I. Salter, N. Leblond, A. Gueneugues, and S. Blain. 2015. Export fluxes in a naturally iron-fertilized area of the Southern Ocean—Part 1: Seasonal dynamics of particulate organic carbon export from a moored sediment trap. Biogeosciences **12**: 3153–3170. doi:10.5194/bg-12-3153-2015

Rembauville, M., and others. 2017. Plankton assemblage estimated with BGC-Argo floats in the Southern Ocean: Implications for seasonal successions and particle export. JGR Oceans **122**: 8278–8292. doi:10.1002/2017JC013067

Roberts, D. W. 2019. labdsv: Ordination and multivariate analysis for ecology. R Package Version 2.-0-1. https://CRAN.R-project.org/package=labdsv

Salazar, G., F. M. Cornejo-Castillo, V. Benítez-Barrios, E. Fraile-Nuez, X. A. Álvarez-Salgado, C. M. Duarte, J. M. Gasol, and S. G. Acinas. 2016. Global diversity and biogeography of deep-sea pelagic prokaryotes. ISME J. **10**: 596–608. doi:10.1038/ismej.2015.137

Shafiee, R. T., J. T. Snow, Q. Zhang, and R. E. M. Rickaby. 2019. Iron requirements and uptake strategies of the globally abundant marine ammonia-oxidising archaeon, *Nitrosopumilus maritimus* SCM1. ISME J. **13**: 2295–2305. doi:10.1038/s41396-019-0434-8

Shafiee, R. T., P. J. Diver, J. T. Snow, Q. Zhang, and R. E. M. Rickaby. 2021. Marine ammonia-oxidising archaea and bacteria occupy distinct iron and copper niches. ISME Commun. **1**: 1. doi:10.1038/s43705-021-00001-7

Sow, S. L. S., and others. 2022. Biogeography of Southern Ocean prokaryotes: A comparison of the Indian and Pacific sectors. Environ. Microbiol. **24**: 2449–2466. doi:10.1111/1462-2920.15906

Sunda, W. G., S. A. Huntsman, and G. R. Harvey. 1983. Photoreduction of manganese oxides in seawater and its geochemical and biological implications. Nature **301**: 234–236. doi:10.1038/301234a0

Sunda, W. G., and S. A. Huntsman. 1994. Photoreduction of manganese oxides in seawater. Mar. Chem. **46**: 133–152. doi:10.1016/0304-4203(94)90051-5

Thi Dieu Vu, H., and Y. Sohrin. 2013. Diverse stoichiometry of dissolved trace metals in the Indian Ocean. Sci. Rep. **3**: 1745. doi:10.1038/srep01745

Acknowledgments

We thank the captain A. Eyssautier, LDA and GENAVIR officers, engineers, technicians, and the crew of the R/V Marion Dufresne for their enthusiasm and their professional assistance during the *SWINGS* cruise. The *SWINGS* project was supported by the Flotte Océanographique Française (10.17600/18001925), Agence Nationale de la Recherche (ANR 19-CE01-0012), CNRS/INSU (Centre National de la Recherche Scientifique/Institut National des Sciences de l'Univers) through its LEFE actions, Université de Bretagne Occidentale, and IsBlue project, Interdisciplinary Graduate School for the Blue Planet (ANR 17-EURE-0015), and co-funded by a grant from the French government under the program "Investissements d'Avenir" embedded in France 2030. We thank Carina Bunse who shared the code for PLSr. We thank the French Institute of Bioinformatics (IFB; https://www.france-bioinformatique.fr) for providing computing resources. We thank two anonymous reviewers and the associate editor for thoughtful comments on a previous version of the manuscript. This work is part of the PhD thesis of R.Z. supported by the China Scholarship Council (CSC; 202006220057).

Conflict of Interest

None declared.

Submitted 20 November 2023
Revised 22 July 2024
Accepted 02 August 2024